Scanning Calorimetric Detections of Multiple DNA Biomarkers Contained in Complex Fluids

ARTICLE *in* ANALYTICAL CHEMISTRY · FEBRUARY 2010

Impact Factor: 5.64 · DOI: 10.1021/ac902503j · Source: PubMed

5 AUTHORS, INCLUDING:

Chaoming Wang
Southwest Jiaotong University
36 PUBLICATIONS **233** CITATIONS

SEE PROFILE

Anal. Chem. **2010,** *82,* 1838–1843

Scanning Calorimetric Detections of Multiple DNA Biomarkers Contained in Complex Fluids

Chaoming Wang,[†,‡] Liyuan Ma,[†] Li-Mei Chen,[§] Karl X. Chai,[§] and Ming Su*[,†,‡]

NanoScience Technology Center, Department of Mechanical, Materials, and Aerospace Engineering, and Biomolecular Science Center, University of Central Florida, Orlando, Florida 32826

Most of the existing techniques cannot be used to detect molecular biomarkers contained in complex fluids due to issues such as enzyme inhibition or signal interference. We have developed a nanoparticle-based scanning calorimetric method for the highly sensitive detections of multiple DNA biomarkers contained in cell lysate and milk by using solid−liquid phase change nanoparticles as thermal barcodes. The detection is based on the principle that the temperature of solid will not rise above the melting temperature unless all solid is molten, thus nanoparticles have sharp melting peaks during the thermal scan process. A one-to-one correspondence can thus be created between one type of nanoparticles and one type of biomarker, i.e., multiple biomarkers can be detected at the same time using a combination of nanoparticles. The melting temperature and the heat flow reflect the type and the concentration of the biomarker, respectively. The target oligonucleotides at low concentration in cell lysate (80 pM) have been detected through thermal signal transduction. The melting temperature of nanoparticles can be designed to avoid interference from coexisting species contained in the fluids, bringing simultaneously high sensitivity and multiplicity, as well as sample preparation benefits to biomarker detections.

Current in vitro cancer detections and diagnosis are strongly dependent on biopsies, where tissue samples are removed from patients for analysis. Although effective in preparing samples, such invasive methods are not suitable for monitoring cancer development and treatment effects. Some cancer cells can exfoliate from the original tumors and enter the circulations and provide an alternative way for the noninvasive or less-invasive detection and diagnosis. It is challenging, however, to detect circulating tumor cells because of their extremely low concentration (1−10 cancer cells in 1 mL blood).[1−3] As a result of fragmentation of the chromatin from dying tumor cells, tumor cells can release molecular biomarkers (i.e., DNAs and proteins) into the circulation. The circulating DNAs reflect the molecular level changes of tumors such as methylation, microsatellite instability, and point mutation and can be used for highly sensitive and less-invasive cancer detections.[4−6] In addition to less invasiveness, detecting molecular biomarkers in body fluid or cell lysate offers many benefits such as minimal sample preparation, more retention of target molecules, low cost, and short analysis time.[7−13]

Although polymerase chain reaction (PCR) and enzyme-linked immunosorbent assay (ELISA) have shown extremely high sensitivities for biomarker detection, these techniques cannot always be used to complex fluids such as cell lysate.[14,15] The application of such techniques is limited in the point-of-care due to sample preparation, equipment maintenance, and needs for skilled personnel.[16] A variety of nanoparticles with unique optical, electric, magnetic, or electrochemical property have been used for in vitro detections of biomarkers.[17−23] By converting biological recognition events into physical signals that can be amplified, nanoparticle based methods achieve high sensitivity at the picomol/liter level owing to intimate contact with biomarkers in solution. However, these methods (except magnetic nanoparticle) require extensive sample preparation effort prior to detection. Otherwise, errors associated with sample preparation could be

* Author to whom correspondence should be addressed. E-mail: mingsu@mail.ucf.edu.

[†] NanoScience Technology Center.

[‡] Department of Mechanical, Materials, and Aerospace Engineering.

[§] Biomolecular Science Center.

(1) Sawyer, C. L. *Nature* **2008**, *452*, 548.
(2) Ferrari, M. *Nat. Rev. Cancer* **2005**, *5*, 161.
(3) Jain, K. K. *Curr. Opin. Mol. Ther.* **2007**, *9*, 563.
(4) Danila, D. C.; Heller, G.; Gignac, G. A.; Gonzalez-Espinoza, R.; Anand, A.; Tanaka, E.; Lilja, H.; Schwartz, L.; Larson, S.; Fleisher, M.; Scher, H. I. *Clin. Cancer Res.* **2007**, *13*, 7053.
(5) Zheng, S.; Lin, H.; Liu, J. Q.; Balic, M.; Datar, R.; Cote, R. J.; Tai, Y.-C. *J. Chromatogr., A* **2007**, *1162*, 154.
(6) Nagrath, S.; Sequist, L. V.; Maheswaran, S.; Bell, D. W.; Irimia, D.; Ulkus, L.; Smith, M. R.; Kwak, E. L.; Digumarthy, S.; Muzikansky, A.; Ryan, P.; Balis, U. J.; Tompkins, G.; Haber, D. A.; Toner, M. *Nature* **2007**, *450*, 1235.
(7) Maraldo, D.; Garcia, F. U.; Mutharasan, R. *Anal. Chem.* **2007**, *79*, 7683.
(8) Paul, B.; Dhir, R.; Landsittel, D.; Hitchens, M. R.; Getzenberg, R. H. *Cancer Res.* **2005**, *15*, 4097.
(9) Acharya, G.; Chang, C.-L.; Doorneweerd, D. D.; Vlashi, E.; Henne, W. A.; Hartmann, L. C.; Low, P. S.; Savran, C. A. *J. Am. Chem. Soc.* **2007**, *129*, 15824.
(10) Bertram, H. C.; Eggers, N.; Eller, N. *Anal. Chem.* **2009**, *81*, 9188.
(11) Xiang, F.; Anderson, G. A.; Veenstra, T. D.; Lipton, M. S.; Smith, R. D. *Anal. Chem.* **2000**, *72*, 2475.
(12) Lazar, I. M.; Trisiripisal, P.; Sarvaiya, H. A. *Anal. Chem.* **2006**, *78*, 5513.
(13) Yang, W.; Sun, X.; Wang, H.-Y.; Woolley, A. T. *Anal. Chem.* **2009**, *81*, 8230.
(14) Griep, M.; Whitney, S.; Nelson, M.; Viljoen, H. *AIChE J.* **2006**, *52*, 384.
(15) Pita, M.; Cui, L.; Gaikwad, R. M.; Katz, E.; Sokolov, I. *Nanotechnology* **2008**, *19*, 375502.
(16) Walt, D. R. *Science* **2005**, *308*, 217.
(17) Mani, V.; Chikkaveeraiah, B. V.; Patel, V.; Gutkind, J. S.; Rusling, J. F. *ACS Nano* **2009**, *3*, 585.
(18) Huang, X. H.; Jain, P. K.; El-Sayed, I. H.; El-Sayed, M. A. *Nanomedicine (London, U. K.)* **2007**, *2*, 681.
(19) White, K. A.; Rosi, N. L. *Nanomedicine (London, U. K.)* **2008**, *3*, 543.
(20) Alivisatos, P. *Nat. Biotechnol.* **2004**, *22*, 47.
(21) Nam, J. M.; Thaxton, C. S.; Mirkin, C. A. *Science* **2003**, *301*, 1884.
(22) Park, S.-J.; Taton, T. A.; Mirkin, C. A. *Science* **2002**, *295*, 1503.
(23) Wang, J.; Liu, G.; Engelhard, M. H.; Lin, Y. *Anal. Chem.* **2006**, *78*, 6974.

10.1021/ac902503j
Published on Web 02/10/2010

large, which will compromise their high sensitivities. For example, colored species in body fluid (i.e., red blood cell) have to be removed for optical detection; pH or salt concentration may affect the electric or electrochemical signals of nanoparticles; although magnetic signals are immune to impurities contained in samples, the signals cannot be amplified readily, and the detection sensitivity is not as high as others.[24−26]

The multistage growth of cancers is characterized by gradual accumulations of molecular genetic abnormalities associated with a range of dynamic processes such as cell cycles, senescence, apoptosis, cellular repair, differentiation, and migration.[27] The diversity of cancers, combined with the complexity of each biological system, makes it difficult to detect molecular biomarker in biofluids.[28] At the early stages, biomarkers are at low concentrations and cannot be detected readily. The medical decision based on a single biomarker has a high probability of false positive and false negative.[29] Thus, single biomarkers alone are not effective for accurate diagnosis. One effective way to enhance the accuracy of a diagnosis is to detect multiple biomarkers from the same sample.[30,31] In one example, 3 to 5 biomarkers can provide more than 0.94 accuracy compared with single biomarkers.[32] Since the amount of sample obtained from a patient is limited, and the quantity of biomarkers is very low, it is desirable to detect multiple cancer biomarkers from one sample using a highly sensitive and multiplexed method.

We have developed a method to detect short single stranded oligonucleotides (ssDNAs) in bodily fluids using solid−liquid phase changes of nanoparticles (Figure 1). The signal transduction is based on the thermal properties of nanoparticles by utilizing a well-known, but unexplored phenomenon, namely, the temperature of a bulk solid will not rise above its melting temperature until the solid becomes liquid completely. In the thermal test, the nanoparticle probes will melt at a narrow temperature range. The position of sharp melting peak and related heat flow are dependent on the nature of the phase change nanoparticles, and the amount of biomarkers in solution, and thus can be used for the qualitative and quantitative biomarker detection. A combination of nanoparticles with different melting temperatures can be used to detect multiple biomarkers with a high level of multiplicity. Since the melting points of nanoparticles can be designed above the melting temperatures of species contained in bodily fluids, the thermal nanoparticles can be used to directly detect molecular biomarkers in bodily fluids. The detection signals are readout using a power compensation differential scanning calorimetry (DSC), in which the heat flow added into a sample to keep its temperature the same as a reference is plotted as a function of temperature. The thermal signal transduction mechanism has no macroscopic analog but brings high sensitivity and multiplicity as well as sample preparation benefits to the area of biomarker detections. Compared to normal microcalorimetry of biological interactions, this approach has higher sensitivity, multiplicity, and specificity owing to the existence of thermal nanoparticles.

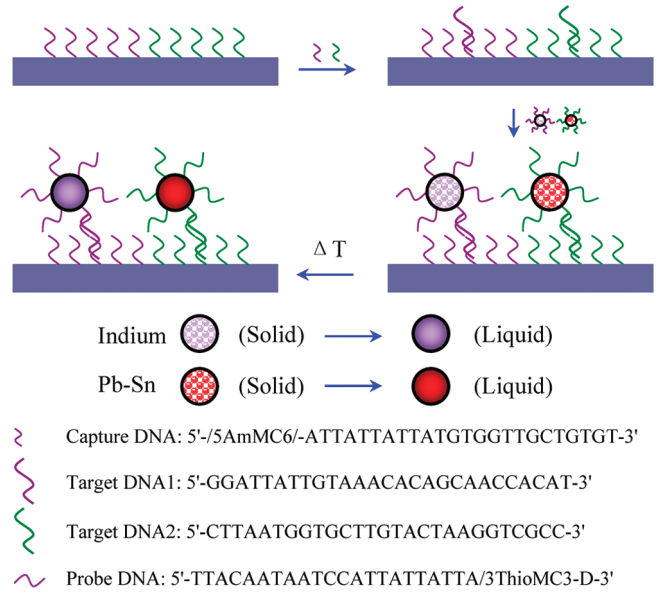

Figure 1. Detecting multiple DNA biomarkers using phase change nanoparticles.

EXPERIMENTAL SECTION

Nanoparticle Synthesis and Characterization. The phase change nanoparticles of low melting temperature metals and alloys are prepared by the thermal decompositions of organometallic precursors. The precursors, such as indium acetate, lead acetate, and tin acetate are obtained from Aldrich and used without purification. The precursors or their mixtures at desired molar ratio and polyvinylpyrrolidone (with molecular weight of 11000) are dissolved in ethylene glycol (Aldrich). The mixture is refluxed at 200 °C to decompose precursors under nitrogen protection. After reacting for 20 min, the reaction is quenched by pouring the mixture in 200 mL of ethanol precooled at 0 °C. The as-prepared nanoparticles are centrifuged at 3000 rpm to remove unreacted precursors and washed by absolute ethanol for three times. A Zeiss Ultra 55 scanning electron microscope (SEM) at an accelerating voltage of 10 kV is used to image nanoparticles dispersed from suspension onto a conductive silicon surface. The compositions of nanoparticles are analyzed by an energy dispersive X-ray (EDX) detector. A JEOL 1011 transmission electron microscope (TEM) operated at 100 kV is used to image the nanoparticles.

Surface Modifications. The synthetic short oligonucleotides are obtained from Integrated DNA Technologies (IDT). The probe ssDNA is 5′-TTACAATAATCCATTATTATTA/3ThioMC3-D-3′; the target ssDNA is 5′-GGATTATTGTAAACACAGCAACCACAT-3′; and the capture ssDNA is 5′-/5AmMC6/-ATTATTATTATGTGGTTGCTGTGT-3′. The sequences of oligonucleotides are designed to be nonspecific for proof-of-principle and are not

(24) Radomska, A.; Eodenszac, E.; Glab, S.; Koncki, R. *Talanta* **2004**, *64*, 603.
(25) Hutton, L.; Newton, M. E.; Unwin, P. R.; Macpherson, J. V. *Anal. Chem.* **2009**, *81* (3), 1023–1032.
(26) Josephson, L.; Perez, J. M.; Weissleder, R. *Angew. Chem., Int. Ed.* **2001**, *40*, 3204.
(27) Kitagawa, D.; Kajiho, H.; Negishi, T.; Ura, S.; Watanabe, T.; Wada, T.; Ichijo, H.; Katada, T.; Nishina, H. *EMBO J.* **2006**, *25*, 3286.
(28) Meyer, H. E.; Stuhler, K. *Proteomics* **2007**, *7*, 18.
(29) Collins, J. M. *J. Clin. Oncol.* **2005**, *23*, 5417.
(30) Wei, F.; Patel, P.; Liao, W.; Chaudhry, K.; Zhang, L.; Arellano-Garcia, M.; Hu, S.; Elashoff, D.; Zhou, H.; Shukla, S.; Shah, F.; Ho, C.-M.; Wong, D. T. *Clin. Cancer Res.* **2009**, *15*, 4446.
(31) Ma, L.; Hong, Y.; Ma, Z.; Kaittanis, C.; Perez, J. M.; Su, M. *Appl. Phys. Lett.* **2009**, *95*, 043701.
(32) Kozak, K. R.; Su, F.; Whitelegge, J. P.; Faull, K.; Reddy, S.; Farisa-Eisner, R. *Proteomics* **2005**, *5*, 4589.

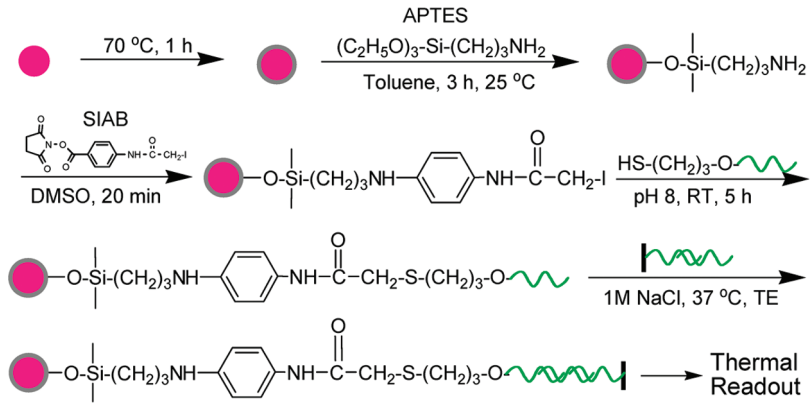

Figure 2. Detailed procedures of surface modification and DNA hybridization.

representative of any biomarkers. Figure 2 shows the procedure of modifying the surfaces of phase change nanoparticles and DNA hybridization. The nanoparticles are modified with amine-terminated monolayers by adding 3-aminopropyltriethoxy-silane (APTES) into the suspension of nanoparticles in toluene. After reacting for 3 h at the room temperature, extra silane is removed by centrifugation, and nanoparticles are resuspended in dimethyl sulfoxide (DMSO) that contains N-succinimidyl(4-iodoacetyl)aminobenzoate (SIAB) and incubated for 20 min to complete the reaction. The disulfide-containing probe ssDNA is reduced to 3′ thiolated probe ssDNA by incubating with tris(2-carboxyethyl)phosphine (TCEP) at pH 4.5 in tris(hydroxymethyl)aminomethane (TE) buffer at 37 °C for 3 h. After removing excess SIAB by centrifugation, the nanoparticles are incubated with the 3′ thiolated probe ssDNA in a phosphate buffer solution (PBS, pH 8.0) at the room temperature. The aluminum surface is modified by APTES in vapor phase, where the surface is kept in a vial that contains 0.1 mL of APTES and heated for 3 h at 100 °C. After washing the surface with DMSO, the aluminum surface is immersed into a DMSO solution of disuccinimidyl suberate (DSS) for 1 h. The surface is washed with PBS and incubated with capture ssDNA in PBS solution (pH 8.0) for 3 h. The hybridization of target ssDNA with capture ssDNA is carried out by immersing the modified aluminum surface in a target ssDNA solution of TE buffer (pH 7.5, 1 M NaCl). After reacting for 3 h at 37 °C, unbounded capture ssDNAs are removed by washing with PBS.

Cell Lysate Preparation. The MDA-MB-231 human breast cancer cells obtained from American Type Culture Collection (ATCC, Manassas, VA) are used. The cells are grown to confluence in T-75 tissue culture flasks using a protocol suggested by ATCC. Then the culture medium is removed, and the cells are washed with the PBS at pH 7.5. The cells are lysed in a 3 mL flask with lysis buffer for 15 min at 4 °C with gentle rocking, where the lysis buffer is composed of 10 mM Tris-HCl at pH 7.5, 100 mM NaCl, 1 mM EDTA, and 1% Triton X-100. The cell lysate is collected and centrifuged at 12,000 rpm for 10 min at 4 °C to remove debris. The supernatant of the cell lysate is collected and stored in small aliquots at −20 °C until use. The total protein concentration of cell lysate is determined to be 1.1 mg/mL using the DC Protein Assay reagent (Bio-Rad Laboratories, Hercules, CA). Bovine serum albumin is used as the standard.

DSC Measurements. A PerkinElmer DSC (DSC 7) is used to measure the melting temperatures and fusion enthalpies of nanoparticles. For nanoparticle characterization, ~10 mg of nanoparticles is sealed inside an aluminum pan, and the DSC test is carried out from 50 to 250 °C at a ramp rate of 10 °C per minute. An empty aluminum pan is used as reference to measure the difference in the heat flows of sample and reference. Both aluminum pans are washed for several times by ethanol and acetone. The detection sensitivity of the equipment is calibrated by measuring the fusion enthalpy of a known amount of bulk material (i.e., indium). For DNA detections, we have modified the aluminum surface with a monolayer of amine terminated molecules by APTES, because the aluminum surface is covered with a thin layer of native oxide after exposing to ambient atmosphere. The patterned immobilizations of fluorescence labeled bovine serum albumin (BSA) on the amine monolayer through covalent bonds confirm the modifications of aluminum surfaces by APTES (Supporting Information). In order to capture the target ssDNA from samples, DSS is used to the immobilize capture ssDNA on the amine terminated aluminum surfaces.

RESULTS AND DISCUSSION

Phase Change Nanoparticles. The structures, morphologies, and thermophysical properties of indium, and lead−tin alloy nanoparticles have been confirmed by the methods (Supporting Information). Figures S1A and S1B show TEM images of indium and lead−tin nanoparticles, which have uniform size distribution around 100 and 30 nm, respectively. The DSC curves confirm the solid−liquid phase changes of nanoparticles (Supporting Information Figures S1C and S1D). Although it has been found that nanoparticles with a diameter smaller than the critical diameter (~40 nm) melt at lower temperatures,[33,34] the nanoparticles prepared here have similar melting points as bulk materials due to their large diameters. In order to modify the surfaces, the nanoparticles of indium and lead−tin alloy are dried and baked at 100 °C in an oven for 1 h. This procedure will oxidize the

(33) Mohamed, M. B.; Wang, Z. L.; El-Sayed, M. A. *J. Phys. Chem. A* **1999**, *103*, 10255.
(34) Dippel, M.; Maier, A.; Gimple, V.; Wider, H.; Evenson, W. E.; Rasera, R. L.; Schatz, G. *Phys. Rev. Lett.* **2001**, *87*, 095505.

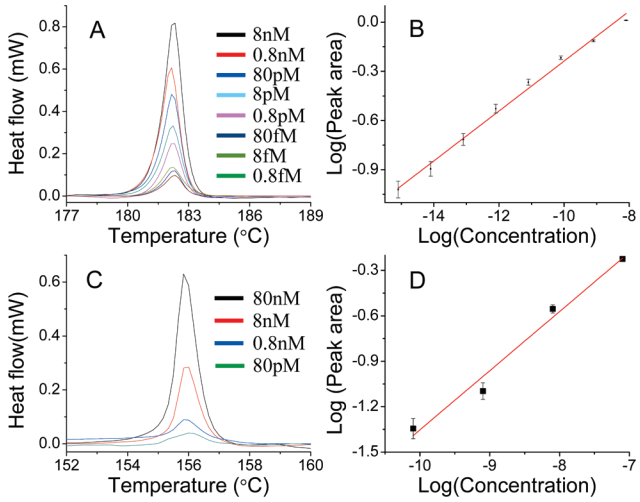

Figure 3. DSC curves of lead−tin nanoparticles captured by target ssDNA at different concentrations in buffer solutions (A), where the concentration of target ssDNA is from 8 nM to 0.8 fM; the relation between target ssDNA concentrations and heat flows of lead−tin nanoparticles (B); DSC curves of indium nanoparticles captured by target ssDNA at different concentrations in buffer solutions (C), where the concentration of target ssDNA is from 80 nM to 80 pM; the relation between target ssDNA concentrations and heat flows of indium nanoparticles (D).

surfaces of low melting nanoparticles (Supporting Information). These nanoparticles are immersed into 5% APTES in toluene for 3 h. After removing extra APTES by centrifuging, nanoparticles are washed by toluene and DMSO. Figure S2A is an EDX spectrum of lead−tin nanoparticles, where the signals of lead, tin, and oxygen can be observed clearly. Furthermore, the oxidization of lead−tin thin film is also confirmed by immobilized fluorescent proteins (Supporting InformationFigure S2B).

DNA Detections in Buffers. Target ssDNAs dissolved in phosphate buffers at pH 8.0 are studied as standard samples for DNA detection. The probe ssDNA modified nanoparticles and capture ssDNA modified aluminum surface are added into the buffer solution for hybridization. After hybridizing for 3 h, the aluminum surface is taken out of the buffer solution, washed by phosphate buffer, and tested by DSC. The standard samples contain a variety of concentrations of target ssDNAs from 8 nM to 0.8 fM in 1 M NaCl and TE buffer. The melting peaks of phase change nanoparticles immobilized through DNA double helix are used for the qualitative and quantitative detections. Figure 3A shows the melting peaks of lead−tin alloy nanoparticles, where the curves from the top to bottom correspond to the concentrations of target ssDNA from 8 nM to 0.8 fM. The areas of melting peaks can be derived by integrating heat flow over the melting range and are proportional to the masses of nanoparticles or the mole numbers of target ssDNA. Figure 3B shows the relation between the peak area and the target ssDNA concentration, where a linear relation exists between the target ssDNA concentration and the peak area, and the lowest detectable concentration is determined to be 0.8 fM. Similarly, indium nanoparticles are used to detect target ssDNAs in buffers. Figure 3C shows the DSC curves of indium nanoparticles collected at different target ssDNA concentrations. Figure 3D shows the relation between the measured peak area and the concentration of ssDNAs, where a linear relation exists between the target ssDNA concentration and the peak area, and the lowest detectable concentration is determined to be 80 pM.

DNA Detections in Complex Fluids. Cell lysate and milk are two biological samples that contain abundant proteins and DNAs. The melting temperature of the phase change nanoparticles made in this experiment is higher than the coexisting species in cell lysate or milk, thus the thermal readout will not be interfered by species in body fluids. But, the DNA hybridization can be affected by abundant proteins or DNAs. Target ssDNAs are added to cell lysate or milk at certain concentrations and detected using the same method described above. The pH values and ion concentrations of cell lysate are adjusted to be 10 mM Tris-HCl at pH 7.5, 100 mM NaCl, and 1 mM EDTA. Figure 4A shows the melting peaks of indium nanoparticles after detecting the target ssDNAs, where the curve from the top to bottom are collected at the concentrations of target ssDNA ranging from 8 nM to 80 pM. Although the temperature range is from 50 to 200 °C, the most parts of curves do not show any heat absorbing behaviors, thus only the thermal behavior in the range from 144 to 168 °C is displayed. Figure 4B shows the relation between the peak area and the concentration of target ssDNA, from which the lowest detectable concentration is determined to be 80 pM. There exists a linear relation between target ssDNA concentrations and heat flows at relatively higher concentrations. Furthermore, the target ssDNA is added in fresh milk to make samples that are not transparent and detected by the same method. The pH values and ion concentrations of milk are adjusted to 10 mM Tris-HCl at pH 7.5, 100 mM NaCl, and 1 mM EDTA. Figure 4C shows the DSC curves of lead−tin nanoparticles that are collected at different concentrations of target ssDNAs, where the melting peaks are attributed to immobilized lead−tin nanoparticles. Figure 4D shows the relation between the measured peak area and the concentration of target ssDNA after detecting target ssDNAs from milk.

Comparison of DNA Detections in Buffers and Complex Fluids. Compared to buffer solutions with clearly defined composition, cell lysate and milk contain abundant proteins; meanwhile, cell lysate could also contain unremoved double-stranded DNA due to disintegration of the nuclear membrane. The proteins or DNAs can affect the detections of the target ssDNAs through either specific interaction or nonspecific adsorption. We have compared the peak areas measured at different concentrations of the target ssDNAs in buffer, cell lysate, and milk. The similar level in response of heat flow means that target ssDNA has been detected. However, there are some differences in the magnitudes of peak areas: peak areas derived from the buffer solutions is similar to those from milk, suggesting that the abundant proteins (1.1 mg/mL) do not affect the hybridization of the target ssDNA very much. Instead, the heat flows measured from the cell lysate are about 20% higher than that from buffer and milk. In the cell lysis process, we have used Triton X-100 as the detergent agent to break cell membrane, which might also break the nucleus membrane and release some DNAs into the cell lysate. It is possible some of the released DNA with sticky ends may interact with the capture ssDNA and probe ssDNA, causing the increased heat flows.

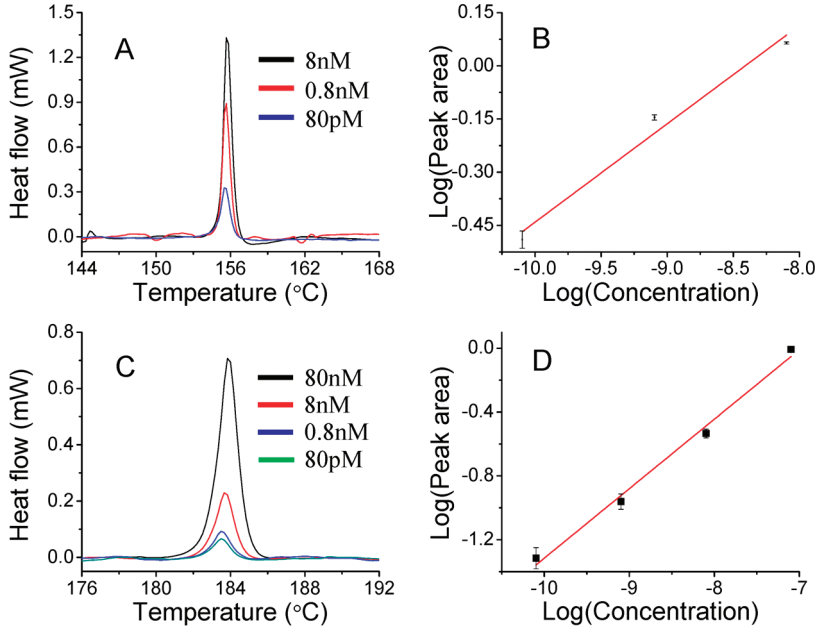

Figure 4. DSC curves of indium nanoparticles captured by target ssDNA at different concentrations in cell lysate (A), where the concentration of target ssDNA is from 8 nM to 80 pM; the relation between the target ssDNA concentration and peak areas of indium nanoparticles (B); DSC curves of lead−tin nanoparticles captured by target ssDNA at different concentration in milk (C), where the concentration of target ssDNA is from 80 nM to 80 pM; the relations between the target ssDNA concentration and peak areas of lead−tin nanoparticles (D).

Detecting Multiple DNA Biomarkers. The sharp and discrete melting peaks of nanoparticles allow the establishment of a one-to-one correspondence between the melting peaks of nanoparticles and biomarkers, thus the method has high multiplicity. We have used this method to detect two different target ssDNAs simultaneously by modifying capture and probe ssDNAs on aluminum surfaces and two types of nanoparticles (i.e., indium and lead−tin alloy). The sequence of the first target ssDNA (ssDNA1) used to modify indium nanoparticles is the same as described above, and the sequence of the second ssDNA (ssDNA2) to modify lead−tin nanoparticles is 5′-CTTAATGGTGCTTGTACTAAGGTCGCC-3′. The capture and probe ssDNAs for the second target have the complementary sequences to each end of the second target. We have mixed the two capture ssDNAs at 1:1 molar ratio and immobilized them on one aluminum pan. Meanwhile, two target ssDNAs are dispersed in TE at pH of 7.5 and 1 M NaCl. The probe ssDNA modified indium and lead−tin nanoparticles and the capture ssDNA modified aluminum surfaces are immersed into the TE that contains two types of target ssDNAs for 3 h. After DNA hybridization, the aluminum surface is washed with a phosphate buffer and tested by DSC. Figure 5A shows the melting peaks of indium, and alloy nanoparticles covalently bonded on aluminum surfaces, thus confirming the existence of two types of target ssDNA in the solution.

Nanoparticle Dependent Sensitivity. The detection sensitivity is dependent on the mass and the latent heat of fusion of nanoparticles as well as the lowest detectable heat flow of DSC. The heat flow (Q) can be derived from the mass (m), the specific heat (C_p) of phase change nanoparticles, and the ramp rate (β) of DSC measurement using the following equation

$$Q = m \cdot C_p \cdot \beta \qquad (1)$$

For indium nanoparticles, the latent heat of fusion is 28.5 kJ/kg. In the case of lead−tin alloy nanoparticles, the latent heat is derived to be 45 kJ/kg using $H = xH_a + (1 - x)H_b$, where H_a and H_b are the latent heats of two metals, and x is the mass ratio of metal A in the alloy. The minimal detectable heat flow in DSC is determined by its root-mean-square noise (0.2 μW), which corresponds to an energy flow of 0.2 μJ for 1 °C wide melting peak at ramp rate of 1 °C/s. Assuming that nanoparticles have uniform diameters (D), and the grafting density of DNA on nanoparticle is α, the minimal number of the target ssDNA (n) that can be detected will be derived from

$$n = \frac{3Q\alpha}{4\pi r^3 \rho C_p \beta} \qquad (2)$$

where r is the radius of nanoparticle, C_p and ρ are the specific heat and the density of nanoparticles, respectively, and β is the ramp rate. From the equation, nanoparticles with large diameter or large latent heat correspond to high sensitivity. Figure 5B shows the relation between peak areas and target ssDNA concentrations for indium and lead−tin nanoparticles. The peak areas corresponding to indium are larger than those of lead−tin nanoparticles, which could be induced by the size difference and grafting density difference of two types of nanoparticles. Equation 2 also shows that lower grafting density corresponds to less target ssDNA or higher detection sensitivity. In our previous experiment on silica encapsulated indium nanoparticles, the lowest detection limit is ~8 nM because the grafting density of DNA on silica layer is higher. As a comparison, the slightly oxidized nanoparticles have lower grafting density of probe ssDNA, thus higher detection sensitivity. Providing there is only one probe ssDNA immobilized on each nanoparticle, the lowest detectable number

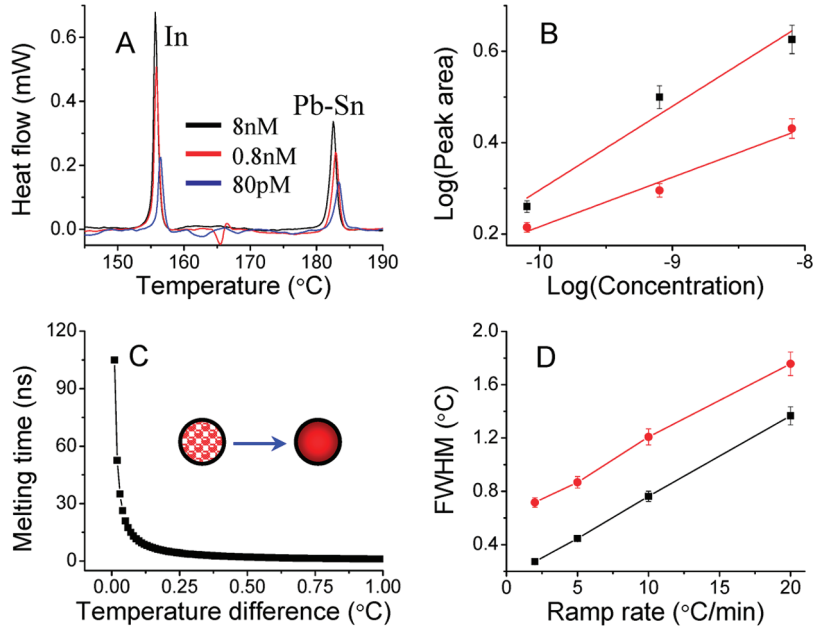

Figure 5. Detecting target ssDNA in cell lysate using indium and lead−tin nanoparticles as probes (A), the concentrations of target ssDNA is at 8 nM, 0.8 nM, and 80 pM, respectively; the relations between peak areas and target ssDNA concentrations for indium (square) and lead−tin (circle) nanoparticles (B); the melting times of indium nanoparticles with diameter of 100 nm as the function of the temperature difference between surface and melting temperature (C); the ramp rate dependent peak width for indium (square) and lead−tin alloy (circle) nanoparticles (D).

of target ssDNA has been estimated to be 0.37 *femto*-mole using indium nanoparticles under the following conditions: r is 50 nm, β is 1 °C/s, Q is 0.2 μW, and C_p and ρ are 0.233 kJ/kg·K and 7310 kg/m^3, respectively.

Multiplicity and Peak Width. The multiplicity of this detection method depends on the widths of melting peaks and the number of different types of nanoparticles. Not only the nanoparticles of pure metals can be used, binary or ternary alloys can be designed based on phase diagrams and produced to offer multiple types of nanoparticles. We have prepared binary alloy nanoparticles that have controlled melting temperatures (Supporting Information Figure S1B). The peak width is determined by two time constants: τ_i is the instrument time constant that depends on ramp rate, measuring head, atmosphere, and crucibles; τ_s is the sample time constant that is a function of sample mass. The larger sample mass corresponds to larger τ_s. Figure 5C shows the simulated melting time of a 100 nm indium nanoparticle as functions of the difference between the surface temperature and the melting temperature of nanoparticles. From the curves, the melting time is less than 100 μs at the ramp rate of 10 °C per minute and the temperature difference of 0.1 °C. The contribution of nanoparticle melting on peak width is smaller than those taken by instrument. Figure 5D shows ramp rate dependent full width at half-maximum (fwhm) of melting peaks measured for indium and alloy nanoparticles. In both cases, the peak width becomes smaller as the ramp rate is decreased. A linear relation exists between ramp rate and peak width, and the smallest peak width among all ramp rates studied is 0.3 °C. Therefore, providing a sufficient number of different alloy nanoparticles can be made with controlled melting temperatures, the multiplicity of this method can be as high as 1000 for the temperature scan range of 100 to 700 °C.

CONCLUSIONS

We have shown the capability of thermally addressed nanoparticles for the detection of molecular biomarkers by using phase change nanoparticles of metallic materials (i.e., pure metal and alloy). The novel signal transduction mechanism allows the detections of multiple DNA biomarkers in cell lysate and milk with high sensitivity, which is comparable to other nanoparticle based methods. In addition, the melting peaks and fusion enthalpies measured from the temperature scan processes can be used for the qualitative and quantitative detections of biomarkers.

ACKNOWLEDGMENT

This work has been supported by the National Sciences Foundation (CBET, grant number 0828466), James & Esther King Biomedical Program of Florida Department of Health, and Air Force Research Laboratory. Most of the characterization work has been performed in Materials Characterization Facility (MCF) at the University of Central Florida (UCF). The nanoparticles are made by Mr. Yan Hong, and the immobilizations of proteins on micropatterns are carried out by Mr. Zeyu Ma. C. Wang and L. Ma contributed equally to this work.

SUPPORTING INFORMATION AVAILABLE

The morphologies and thermophysical properties of indium and lead−tin alloy nanoparticles have been confirmed by the TEM and DSC (Figure S1) and the component of bare and modified aluminum or nanoparticles surface (Figure S2). This material is available free of charge via the Internet at http://pubs.acs.org.

Received for review November 3, 2009. Accepted January 26, 2010.

AC902503J